Characterisation of vertical BrO distribution during events of enhanced tropospheric BrO in Antarctica, from combined remote and in-situ measurements

H.K. Roscoe [a,*], N. Brough [a], A.E. Jones [a], F. Wittrock [b], A. Richter [b], M. Van Roozendael [c], F. Hendrick [c]

[a] British Antarctic Survey, Cambridge, UK
[b] IUPP, University of Bremen, Germany
[c] BIRA, 3 Ave Circulaire, Brussels, Belgium

ARTICLE INFO

ABSTRACT

Tropospheric BrO was measured by a ground-based remote-sensing spectrometer at Halley in Antarctica in spring 2007, and BrO was measured by satellite-borne remote-sensing spectrometers using similar spectral regions and similar Differential Optical Absorption Spectroscopy (DOAS) analyses. Near-surface BrO was simultaneously measured in situ at Halley by Chemical Ionisation Mass Spectrometer (CIMS), and in an earlier year near-surface BrO was measured at Halley over a long path by a ground-based DOAS spectrometer. During enhancement episodes, total amounts of tropospheric BrO from the ground-based remote-sensor were similar to those from space, but if we assume that the BrO was confined to the mixed layer they were very much larger than values measured by either near-surface technique. This large apparent discrepancy can be resolved if substantial amounts of BrO were in the free troposphere during most enhancement episodes. Amounts observed by the ground-based remote sensor at different elevation angles, and their formal inversions to vertical profiles, demonstrate that much of the BrO was indeed often in the free troposphere. This is consistent with the ∼5 day lifetime of Bry and with the enhanced BrO observed during some Antarctic blizzards.

1. Introduction

In spring in both polar regions, concentrations of tropospheric ozone can decrease rapidly from normal (background) values to almost zero, and remain there for periods of hours to days [1]. These tropospheric ozone depletion events (ODEs) are driven by bromine chemistry, the reactive bromine compounds (Bry) being released from the sea ice zone (e.g. [2,1]). The resultant Br catalytically removes ozone in a cycle involving BrO, a trace gas that can be measured by a variety of techniques.

The oxidising capacity of the polar troposphere is significantly altered by ODEs, during which oxidation is shifted towards control by halogen compounds. Furthermore, if the ozone-poor air can be transported to high enough altitude, or if the BrO or its aerosol sources can be transported to a high enough altitude that it continues to cause ozone depletion aloft, a small radiative effect can occur which would have a positive climate feedback [3].

When using remote sensors to deduce near-surface mixing ratios of trace gases such as BrO, it is necessary to make assumptions about the vertical profile of the gas,

and as BrO is produced at the surface it is a common assumption in such analyses that most BrO resides in the mixed layer. In this paper, we discuss new remote-sensing and in-situ near-surface measurements of BrO in Antarctica, and address a large and important apparent discrepancy between the remote and the in-situ measurements when using this assumption. We compare these measurements to other recent remote-sensing measurements and previous in-situ measurements to show that they also suffer the same large apparent discrepancy. The way our new ground-based remote sensing measurements change with elevation viewing angle leads us to conclude that BrO is frequently in the free troposphere in the Antarctic, which resolves the apparent discrepancy. This conclusion is reinforced by formal profile inversions of our ground-based remote sensing measurements.

There have been earlier measurements and analyses leading to the conclusion of BrO in the polar free troposphere: from an aircraft flight of a remote sensor in the Arctic, McElroy et al. [4] showed good evidence for a potential discrepancy similar to that of this work, and also suggested that it could be resolved if BrO was present in the free troposphere; Parrella et al. [5] speculated about BrO in the free troposphere from satellite remote-sensing measurements. Salawitch et al. [6] showed that MAX-DOAS measurements in the Arctic in April 2008 were consistent with BrO at altitudes above the boundary layer on some days; and at least 7 of 45 profiles measuring BrO with an airborne in-situ sensor in the Arctic during April 2008 observed enhanced BrO in layers above 1 km altitude [7].

However, other Arctic measurements in spring show little BrO in the free troposphere: inversions of MAX-DOAS measurements at Barrow in 2009 by Friess et al. [8] show some enhancements at 0.2 km but very little above 0.5 km (their Fig. 13); near Alert in 2000, Honninger and Platt [9] deduced little uplift of enhanced BrO beyond 1 km; Prados-Roman et al. [10] and Neuman et al. [11] showed negligible free-tropospheric BrO during their aircraft campaign.

Hence the previous evidence for free-tropospheric BrO during polar enhancements was either sporadic or for single days. Here, we build on this previous work to show conclusively that, on many days in the Antarctic spring of 2007, the potential discrepancy is large and that significant amounts of BrO must indeed be in the free troposphere.

2. Measurement techniques

Section 3 discusses Antarctic BrO results in spring from four instruments:

1. ground-based multiple-axis DOAS (MAX-DOAS) spectrometer in 2007;
2. satellite-borne spectrometer Global Ozone Monitor-2 (GOME-2) in 2007;
3. near-surface long path in-situ DOAS spectrometer in 2004; and
4. near-surface local in-situ CIMS in 2007.

These instruments are defined and described below.

2.1. Ground-based MAX-DOAS spectrometers

Sunlight scattered from the sky was observed by a ground-based UV–visible spectrometer, located in Antarctica at Halley V research station (75.6°S, 26.7°W). The spectrometer was positioned on the roof of the clean air sector laboratory (CASLab [12]), 1 km from the main base, to the SE where it receives minimal wind from the base and its generators.

The apparatus consisted of a temperature-controlled insulated box, mounted to a gearbox, motor and magnetic stops that enabled it to scan in elevation. The box contained the spectrometer, a quartz entrance lens and a motor controller, plus electronics to interface the spectrometer and motor controller to a PC inside the laboratory via USB. The box and its bulkhead connectors were sealed, and it contained drying agent to keep the components and window moisture free. The box's proportional temperature controller used up to 30 W of DC power and was set at a value close to 0 °C. This power proved insufficient in stronger winds or the coldest temperatures (< -35 °C) at Halley in early spring, which was of concern because the spectral calibration and resolution of the spectrometer could shift with temperature. Laboratory tests at BIRA with another spectrometer of the same type had shown that the shifts became significantly larger as it was cooled from 0 to -5 °C.

Spectra from the elevation-scanning (so-called Multiple Axis) spectrometer were analysed by Differential Optical Absorption Spectroscopy (the MAX-DOAS technique). Our apparatus was a miniaturised instrument of the Hoffman–Heidelberg design, using an Ocean Optics USB-2000 spectrometer. It was set to average 1000 non-saturating spectra at each elevation angle, taking from 2 to 7 min depending on light intensity. It scanned to elevation angles 2°, 4°, 15° and 90°, the sequence being repeated every 8–30 min, except only 1 in 3 sequences included 90° elevation. The field of view was 0.5°, so the surface snow could not have been seen at 2° elevation unless there were large errors in the scan (see below). It measured at wavelengths from 337 to 481 nm with a spectral resolution of about 0.7 nm. BrO was analysed from 341 to 356 nm, an interval that includes 3 strong lines of BrO, and all of one and part of another O_4 line.

The observed spectrum also contains Fraunhofer lines from the atmosphere of the sun, which would interfere with BrO absorption lines, but because the Fraunhofer lines do not vary with time the observed spectra can be divided by a reference spectrum obtained at a high elevation to remove them. This reference spectrum also contains a small slant amount of NO_2 which by this division becomes subtracted from the actual slant amounts in the observed spectra. The amount of BrO is then found by fitting laboratory cross-sections to the ratio of observed to reference spectrum, after applying a high-pass filter in wavelength to the observed spectral ratio and the laboratory cross sections (the DOAS technique). The interfering trace gases O_3, O_4 and NO_2 are also included in the spectral fit.

Our DOAS analyses were carried out by the BIRA software suite "WinDOAS". This does a separate calibration of wavelength for each spectrum, using the locations of Fraunhofer lines within it compared to those of a high-resolution

solar spectrum by Kurucz [13]. It can also do a separate calibration of spectral response function using the widths of the Fraunhofer lines and of the trace gases, but the weak features of the trace gases in this region led to instabilities in the fits, so this software option was not selected. Hence we were careful to choose reference spectra at instrument temperatures within 0.3 °C of each part-day of low-elevation spectra. The spectral inversion was from 341 to 356 nm using BrO cross sections from Wahner et al. [14], whose wavelengths were shifted by $+0.17$ nm before spectral analysis, as suggested by Aliwell et al. [15] who fully discuss the accuracy of the wavelength calibration. NO_2, O_3 and O_4 are also included in the spectral fit, but not HCHO or OClO.

In MAX-DOAS geometry, the light path through the stratosphere is almost identical in a low-elevation view and the zenith view (e.g. [16]). Hence by using a spectrum of the zenith sky as a reference, the amount of stratospheric BrO is automatically subtracted from the spectrum at lower elevation, at the same solar zenith angle. We used a zenith spectrum near noon within 20 days of the measurement day as a reference, mostly within 10 days. We chose as a reference a day when the temperature of the spectrometer was within 0.3 °C of the measurement day. The spectrometer's thermostat was near the limit of its ability to control temperatures in the very variable external temperatures in our measurement period, and temperatures on some measurements days differed from those on other measurement days by up to 5 °C. If we used a closer reference with a larger temperature difference, the residuals from the spectral fit were too large. A reference near noon on the same day was not an option except on 4 days, either because of cloud despite a sunny morning or afternoon, or because the spectrometer lost synchronisation with its control computer near noon.

We minimise the sensitivity to stratospheric amounts, in the calculation of vertical amounts below, by subtracting the simultaneous zenith amount from the low-elevation slant amounts. As the amount in the zenith view is mostly in the stratosphere and is almost identical to the stratospheric amount in the simultaneous low-elevation view, the subtracted slant amounts are almost entirely tropospheric. We also restrict our measurements to solar zenith angle $< 85°$, which reduces the slant amount in the stratospheric part of the path.

The MAX-DOAS measurements of BrO are those of the slant column (minus the slant column in the reference spectrum), whereas it is the vertical column that is of greater scientific interest. The ratio of the slant path length to the vertical is known as the Air Mass Factor (AMF). Because there is no single path of scattered light, the effective slant paths through the atmosphere must be calculated by a radiative transfer code. Here we used the code "UVspec/DISORT" [17], which has been validated through several intercomparison exercises (e.g. [18]). Our calculations assumed all the BrO was in the lowest 200 m (see below for a discussion of this assumption) and that the aerosol was zero. To account for the tropospheric amount in the reference spectrum, the vertical amount in each low-elevation spectrum was deduced by dividing the slant amount by (AMF (low-elevation)–AMF (zenith)).

Parts of the elevation scanning system (gearbox, magnet, magnetic switches to determine end-stops) were outside the temperature controlled box. During laboratory tests in a freezer at BAS, the magnet and switches were found to vary in sensitivity with temperature such that the elevation could vary by 0.5° between -45 °C and 20 °C. During a field campaign in summer, other scanners of the same design were found to have nominally horizontal views in error by over 1° [19], due to a combination of gearbox wear, hysteresis and errors during setting up. Our spectrometer was mounted on a building on legs, that could be felt to sway in strong winds, and although the arrangement of legs preserved the nominal horizontal of the platform, in an earlier year a distant retro-reflector subtending 0.05° had to be re-centred on a telescope at frequent intervals. Coupled with the field of view of 0.5°, it is therefore just feasible for a view at a nominal 2° elevation to have observed part of the snow at the horizon from time to time, though this is not feasible for views at 4° and above.

2.2. Satellite-borne spectrometer GOME-2

The second Global Ozone Monitoring Experiment (GOME-2) is a UV–visible spectrometer looking downward from space to observe sunlight scattered from the atmosphere and the surface of the Earth [20]. It measures from 240 to 790 nm, with a spectral resolution of 0.2–0.5 nm, and each day a solar spectrum is measured to serve as a reference spectrum during spectral analysis. GOME-2 is on the Meteorological Operational Satellite-A, launched in October 2006 to a sun-synchronous polar orbit with an equator crossing time of 09:30 LT on the descending node. Global coverage is achieved within 3 days at the equator and within 1 day towards the poles.

BrO is found by DOAS analysis, as for our MAX-DOAS in Section 2.1. The results shown below from Theys et al. [21] fitted BrO in the range 332–359 nm, wider towards the UV than that of our MAX-DOAS analysis in order to cover 5 rather than 3 lines of BrO. This helps with nadir measurements from space because of the smaller slant paths than observed by a MAX-DOAS looking close to the horizon.

The analysis by Theys et al. [21] follows earlier work [22] that calculates a rigorous vertical amount of tropospheric BrO by subtracting from the observed total BrO the stratospheric BrO deduced from a chemistry transport model plus correlation with dynamical and chemical indicators, a method adopted and extended by Salawitch et al. [6] and Choi et al. [7]. The remaining tropospheric BrO is then rescaled by a tropospheric AMF, which is often quite different to the stratospheric AMF that was conventionally used to calculate total BrO amounts.

2.3. Near-surface long path in-situ DOAS spectrometer

Between January 2004 and February 2005, the concentration of BrO was measured at Halley by a spectrometer observing a lamp via a distant retro-reflector [23]. Light from the xenon lamp in the CASLab was reflected back to the telescope and spectrometer by an array of quartz

corner cubes at a distance of 4 km. The resulting 8 km sample path was at a height of 4–5 m above the snowpack. Spectra between 324 and 338 nm were analysed for BrO by the DOAS method described in Section 2.1. This interval is at shorter wavelengths than that of our MAX-DOAS because of the larger ratio of UV to visible light from the xenon lamp compared to scattered sunlight.

2.4. Near-surface local in-situ CIMS

The Chemical Ionisation Mass Spectrometer (CIMS) at Halley was based on the method outlined by Huey et al. [24] and Slusher et al. [25], and the wider chemical interpretation of the results is discussed by Buys et al. [26]. The components are an inlet, a reaction chamber, a collisional dissociation chamber, an octopole ion guide plus quadrupole mass spectrometer, and an ion detector. SF_6 is converted to SF_6^- as it passes through an ion source, then mixed with ambient air to react with various trace gases including SO_2 and BrO. The resultant ions are detected one at a time by the mass spectrometer.

A major problem for this technique is interference by water vapour. In a high water environment, water clusters form around the reagent ion, and it is difficult to measure trace gases at concentrations of a few pptv. However, laboratory and field results [25] indicate that at frost points below -25 °C the interference is small. No observable water interference was found at Halley during spring.

At Halley, ambient air was continually sampled at a high flow rate via a Teflon cap and wide aluminium pipe, 5 m above the snow surface. Air from the centre of the pipe was sub-sampled through a heated PFA inlet. The CIMS was operated alternately in two different modes, being switched from one to the other every few weeks:

(a) at high pressure, measuring OH and peroxy radicals; and
(b) at low pressure, measuring trace gases including BrO.

In the low pressure mode, the measurement sequence consisted of integrating the signals sequentially at the various masses corresponding to the wanted ion products, including 95 amu for BrO^-. The sequence was repeated at least every 10 s.

Sensitivity to SO_2 was found by introducing a certified standard for 1 min every 2 h, those of the halogen compounds relative to SO_2 having been previously determined in the laboratory [27]. The zero of the measurement was obtained by filtering the inlet air through activated charcoal, together with dried nylon and glass wool that had been previously soaked in $NaHCO_3$ solution.

3. Results

The calculation of AMF with MAX-DOAS geometry is subject to larger uncertainties with high aerosol loading or significant clouds. Fortunately, high aerosol loading is rare in unpolluted Antarctica, though fog and wind-blown snow are common. In the idealised case of very dense cloud over highly-reflecting snow, the scattering between cloud and snow renders the light fully diffuse so that all elevations see the same scene. The diffuseness occurs at all wavelengths so that the phenomenon must affect the observed O_4 as well as the BrO. In the realistic case of cloud that is not fully opaque, and snow that has the normal albedo of about 0.8, the light is not fully diffuse, but there is nevertheless a tendency to small slant-path differences that are inherently difficult to calculate.

Hence we eliminated cloudy days and cloudy parts of days by choosing only portions with less than or equal to 3 oktas (eighths) cloud, taken from the meteorological log at Halley. We used the size of the O_4 signals to interpolate cloudiness between the 3-hourly meteorological observations. Such cloudy periods were assessed by eye for large changes in O_4 relative to the scatter in the O_4 signals, and eliminated. With one day's exception, we also eliminated observations close to twilight (solar zenith angle $>85°$), because the stratospheric amount can then differ markedly from that of the noon reference, because the interference from stratospheric ozone then becomes very large, and because light intensity then becomes much less. The exception was 25 August, a day early in the season when the CIMS was already operating, and with some completely clear skies – eliminating solar zenith angles of less than 85° would have left almost no data on this day. Periods with rapidly changing spectrometer temperatures were also eliminated for the technical reasons discussed in Section 2.1; this was done by examining plots of spectrometer temperature and removing periods during any one day when it changed by more than 0.3 °C.

Fig. 1 shows two days of measurements of slant amounts, chosen to represent those with larger amounts of cloud (12 Oct.) and small amounts of cloud (13 Oct.). Important features are

(a) There is less O_4 on 12 Oct., because there was more cloud.
(b) Despite using same-day reference spectra for each of the two days, the noise on 12 Oct. is larger. We suspect this is due to the variability of the larger cloud amounts. The noise on the almost cloud-free 13 October was smaller and is likely due to the random error in the spectral fit.
(c) The noise is large enough that some averaging must be done – working with individual elevation scans is not realistic. We chose to use daily medians (see below).
(d) All slant amounts have a tendency to increase with increasing solar zenith angle. This is probably because of interference from stratospheric ozone, not properly accounted for in the spectral inversions, as well as from stratospheric BrO. If they are from stratospheric gases, they should be almost identical at all elevations and so be removed by the subtraction of zenith amounts.

Fig. 2 shows the average over the three elevations (2°, 4°, and 15°) of total vertical tropospheric BrO measured by the MAX-DOAS on the sunny days or part-days, after subtracting the slant amount in the zenith view and dividing by the difference in AMF from that of the zenith view. This
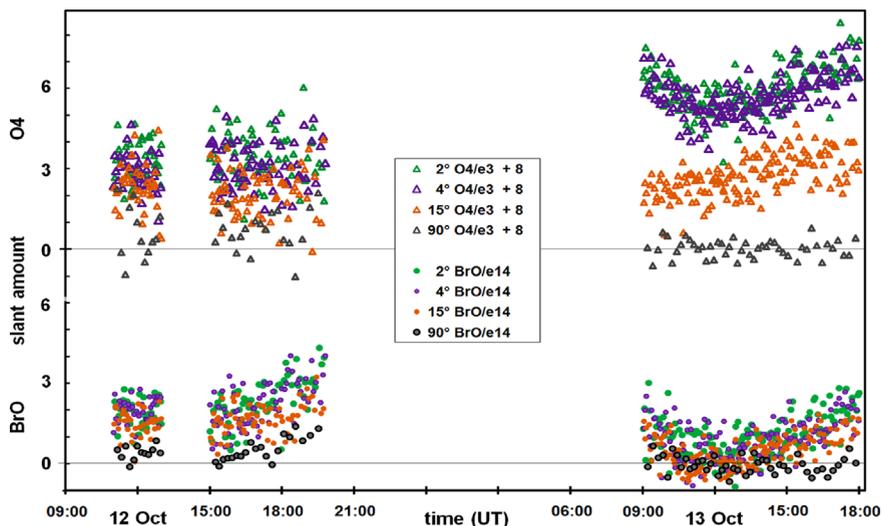
Fig. 1. Individual measurements by MAX-DOAS at Halley in 2007, on two selected days, at the 4 angles of the elevation scan. The lower half shows slant amounts of BrO (units 10^{14} molecule cm^{-2}); the upper half shows slant amounts of O_4 (units 10^3 molecule^2 cm^{-4}). 12 Oct. had more cloud, hence the larger amounts of O_4 (see text); and the cloud was more variable, hence the larger scatter. These are measurements with SZA $< 85°$, so stratospheric BrO is barely discernible in the results.
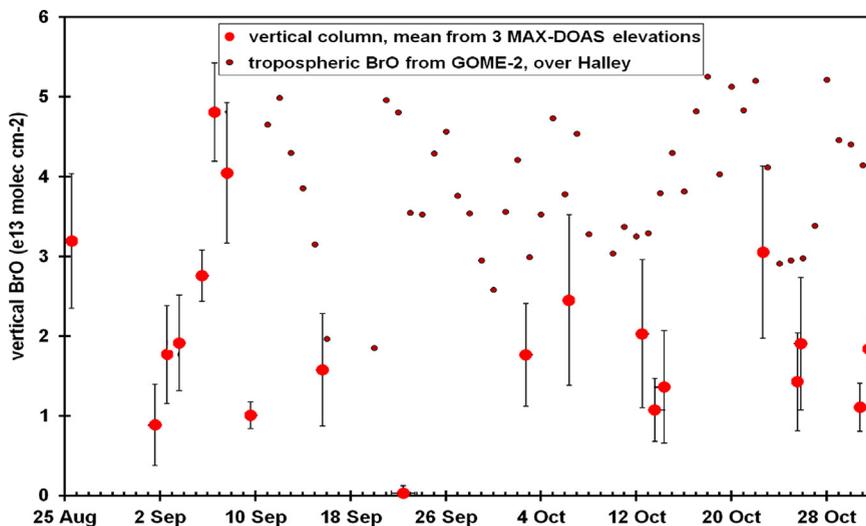
Fig. 2. Vertical tropospheric BrO at Halley in Antarctica in spring 2007. Large red circles: average of the vertical amounts at elevations of 2°, 4° and 15° measured by our MAX-DOAS under the assumption of a 200-m BrO layer near the surface. The measurements are medians of those on each sunny day or part-day (≤ 3 oktas); error bars are the standard error of the average of the three elevations. Small red circles with black rims: GOME-2 data within 200 km of Halley (courtesy Nicolas Theys, see [21]). (For interpretation of the references to colour in this figure legend, the reader is referred to the web version of this article.)

calculation used the median of each day's or part-day's slant columns – we chose median rather than mean because there were some obvious spikes in the raw time series of slant columns (not seen in the days in Fig. 1), presumably due to data drop out, and medians are the simplest way of reducing sensitivity to spikes in data. Drop out was probably because of difficulties with the USB link to the computer, which had to be rebooted frequently until a USB connector on the moving part of the elevation scan was relocated part way through the year.

Although the MAX-DOAS measured BrO from 25 August, 2007 until 5 February, 2008, in Fig. 2 we show just the period

in spring 2007 that overlaps the simultaneous CIMS measurements, plus the following month to illustrate the continuing quality and features of the data. From Fig. 2, we see that the ground-based MAX-DOAS spectrometer apparently observed from 0 to 5×10^{13} molecule cm^{-2} of tropospheric BrO above Halley in spring 2007.

Fig. 2 also shows tropospheric values near Halley from the satellite-borne spectrometer GOME-2, which lie between 2 and 5.5×10^{13} molecule cm^{-2} near Halley in 2007 [21]. Hence GOME-2 values are of similar order of magnitude to our MAX-DOAS values, although they are in general about twice those of MAX-DOAS (note that using
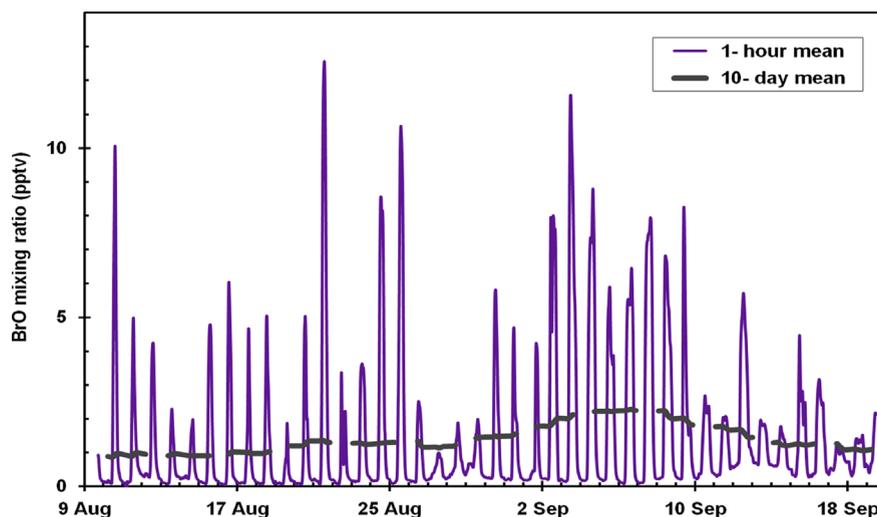
Fig. 3. Measurements of BrO by the CIMS in-situ sampler at Halley in spring 2007. The solid purple line is the 10-min data smoothed by a triangular function of half-width 1 h. The thick grey dashed line is a 10-day running mean of all values, including night-time for ease of comparison with data from Saiz-Lopez et al. [23], and between 10 August and 19 September its value was between 1 and 2.2 pptv. (For interpretation of the references to colour in this figure legend, the reader is referred to the web version of this article.)

these larger GOME-2 values would make the discrepancy discussed below worse). Also, the discrepancy would be resolved either (a) by using the NASA approach for calculation of stratospheric burden in satellite measurements of BrO [6], which places more BrO in the stratosphere because it assumes that most very short-lived Bry entering the stratosphere does so as product gasses, whereas the calculation of Theys et al. [21] assumes most enter as source gasses; or (b) by using only the larger vertical amounts at 15° elevation in our MAX-DOAS values – see the last paragraph in Section 5 for examples.

Fig. 3 shows the CIMS results in spring 2007, which vary between 0 and 12 pptv, and whose 10-day running mean of all values including night-time varies between 1 and 2.2 pptv for the period of CIMS operation (10 August to 19 September). In August and September 2004, long-path DOAS results varied between 0 and 9 pptv, and the 10-day mean of all values including night-time was between 1.5 and 3.5 pptv [23]. Hence these earlier long-path DOAS results are very similar to our recent CIMS values.

4. Interpretation

Section 3 demonstrates that the two remote-sensing instruments, the first on the ground and the second in space, see vertical amounts of tropospheric BrO that lie within a factor of about 2 of one another. Section 3 also demonstrates that the two in-situ sensors observed very similar mixing ratios of BrO in different years; and the comprehensive study by Liao et al. [28] found a similar result from simultaneous measurements by their two in-situ techniques in the Arctic (their Fig. 6). Hence we have good confidence in all the four techniques and analyses.

In order to relate the remote sensing results of vertical column to the in-situ results of mixing ratio, we must assume a vertical distribution of BrO. The simplest and

most widely used (e.g. [29]) is to assume it is equally mixed in a layer at the surface, of thickness equal to the mixed layer height (although Wagner et al. [29] also included calculations for profiles with BrO aloft).

Unfortunately the mixed layer height at Halley sometimes varies hugely over periods of a few hours, despite the flatness of the site and the surrounding ice shelf, probably as a result of fossil inversions being carried large distances by the mean flow [30], plus synoptic weather systems. We examined sodar measurements at Halley, and heights were estimated on days of simultaneous CIMS and MAX-DOAS measurements to vary from 75 to 300 m, with a mean of 140 m. Three of the days also had another layer discernible just above ground clutter, varying in height from 25 to 40 m. To proceed with the comparison, we chose a layer thickness of 200 m as a starting point.

On 6 Sep 2007, the MAX-DOAS vertical column translates to 130 pptv by assuming a layer thickness of 200 m. This is at least 10 times the BrO observed in-situ by CIMS. The scaling is inversely proportional to layer thickness, so a layer thickness of 2 km would be needed to obtain good agreement if the AMF was unchanged, completely unrealistic for the mixed layer at Halley. Fig. 4 compares CIMS results to MAX-DOAS assuming a mixed layer height of 200 m but dividing MAX-DOAS results by 10, to demonstrate the consistency of the discrepancy. Choosing a layer thickness equal to the mean sodar value of 140 m, or equal to that of the lower secondary layer seen by sodar on some days, would make the disagreement worse. Note that in fact the AMF decreases as layer thickness is increased, so that agreement cannot be obtained using a well-mixed layer of thickness about 2 km – the thickness would be much larger. Also note that the discrepancy between the GOME-2 results in Fig. 2 and CIMS would be a factor 20 rather 10.

A similar calculation was made by Wagner et al. [29] for MAX-DOAS measurements of BrO enhancements from
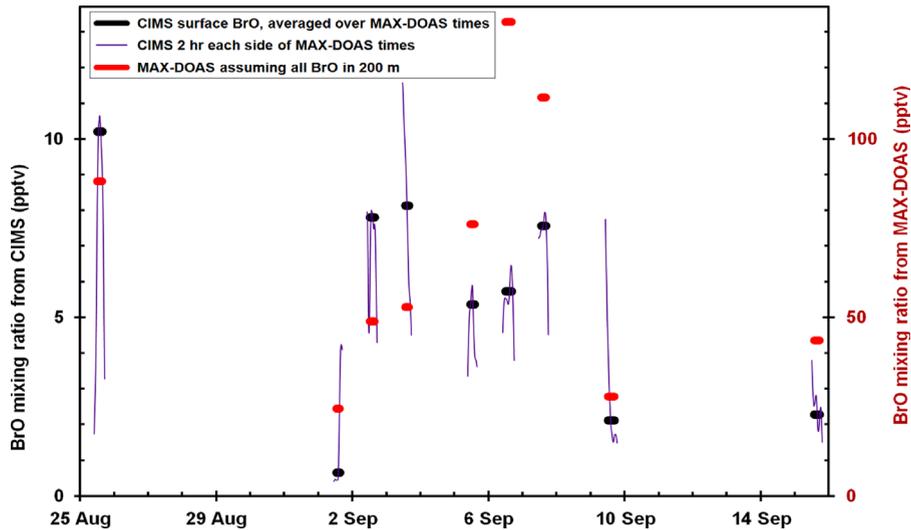
Fig. 4. Medians of each sunny day or part-day of MAX-DOAS BrO, assuming all BrO is confined to a surface layer of thickness 200 m (short thick red lines, right-hand scale), together with the simultaneous mean of CIMS BrO (short thick black lines, left-hand scale), and the 1-h smoothed CIMS BrO up to 2 h before and after the MAX-DOAS measurements (thin purple lines, left-hand scale). The purple lines account for the MAX-DOAS sampling air centred up to 4 km away and if winds were as low as 2 km/h. Purple lines demonstrate that the lack of collocation of MAX-DOAS and CIMS measurements cannot be responsible for the apparent 10-fold discrepancy between them. (For interpretation of the references to colour in this figure legend, the reader is referred to the web version of this article.)
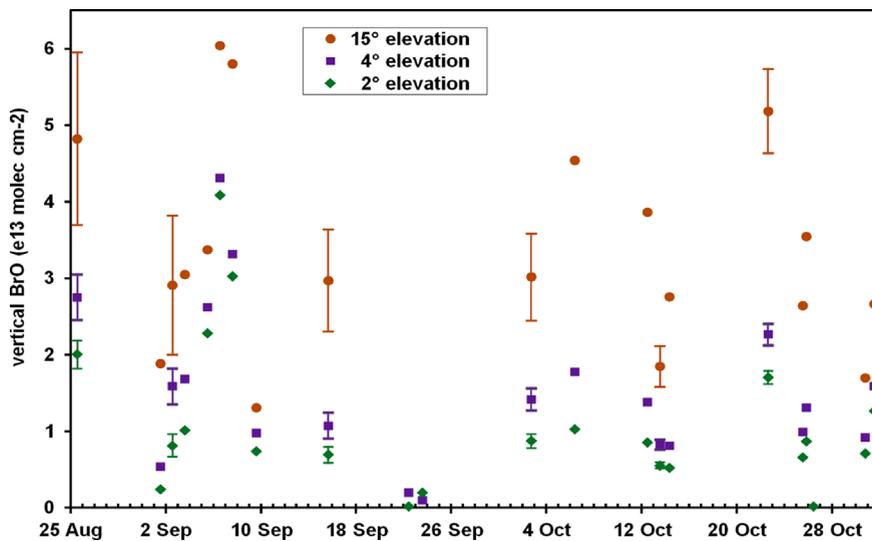
Fig. 5. Vertical tropospheric BrO measured at Halley in Antarctica in spring 2007 by MAX-DOAS, at each elevation angle, shows the cause of the discrepancy in Fig. 4. The air mass factors assume that all the BrO is in the lowest 200 m: the differences between elevations show this assumption is not correct. Estimates of $1-\sigma$ error bars are shown at some points (all error bars would overly clutter the plot), showing that the differences are significant. Errors at later dates are smaller due to the increasing duration of daylight. These are medians of each sunny day or part-day.

a ship in the Weddell Sea in 2006. Their Table 1 converts a slant column of 10^{15} molecule cm^{-2} at 1° elevation to 50 pptv in a mixed layer of thickness 200 m. Our slant column difference from 90° at 2° elevation on 6 September was 0.8×10^{15} molecule cm^{-2}, which at 1° elevation would be a slant column difference of about 1.5×10^{15} molecule cm^{-2}, and our result is 130 pptv – hence our conversion factor is similar to that derived by Wagner et al. [29].

Wagner et al. [29] also noted that their MAX-DOAS measurements were equivalent to unrealistically large mixed-layer BrO mixing ratios, but they refrained from suggesting that there was in fact a discrepancy with previous Antarctic in-situ measurements. They did show from their calculations with a variety of profile shapes that the maximum BrO is probably located above the mixed layer in some of their measurements.

Because of its remote-sensing geometry, MAX-DOAS observes up to several km away from its site, so our simultaneous comparison with in-situ results could be rendered void. However, on 5 of the 9 days for which
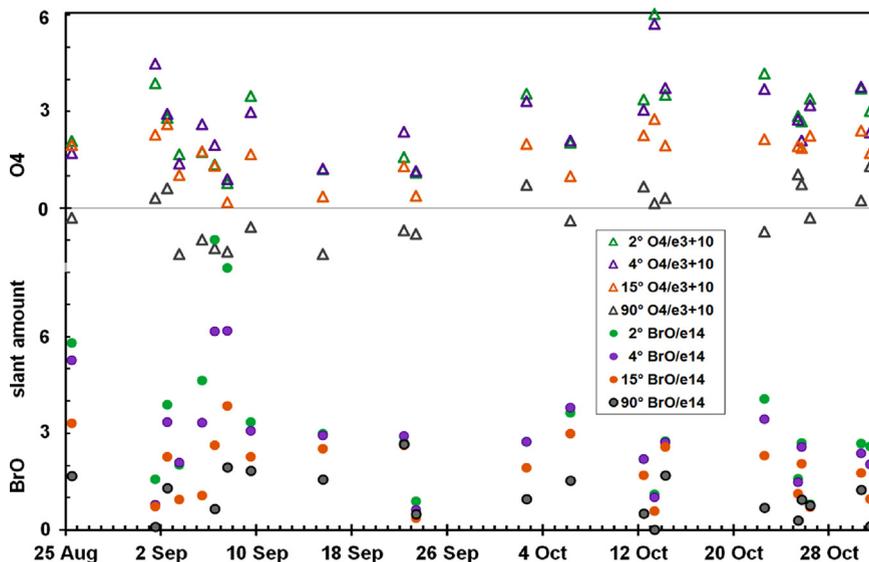
Fig. 6. Slant amounts of BrO and O_4 measured at Halley in Antarctica in spring 2007 by MAX-DOAS at the elevations observed (units as Fig. 1). These are medians of each sunny day or part-day. The reference spectrum was often on a nearby rather than the same day, hence the non-zero values at 90°.

there are simultaneous MAX-DOAS and CIMS results, Fig. 4 shows that CIMS results are a maximum (i.e. closest to MAX-DOAS) at the times of the MAX-DOAS measurements. Hence the discrepancy would be larger if the air sampled by CIMS was observed by MAX-DOAS earlier or later.

The inescapable conclusion is that large amounts of BrO must frequently lie above 200 m during observations of Antarctic enhancement episodes at near-coastal sites such as Halley, and from Wagner et al. [29] over the sea ice zone. As 200 m can be taken as a representative height of the mixed layer at Halley, much of the BrO must often be in the free troposphere.

This conclusion is borne out by the variation of our MAX-DOAS vertical and slant columns with elevation angle. Fig. 5 shows that the vertical column appears much larger at 15° elevation angle than at 2° or 4° on most days in spring with enhanced BrO, in excess of the approximate errors also shown in Fig. 6. This is only possible if the AMFs are incorrect because much of the BrO in fact lies well above 200 m.

The calculation of the approximate errors in Fig. 6 is problematic. In fact there is no formal error for the median of a data set, unlike for the mean. We determined standard deviations of each day's slant columns, and looked at their minima, on the assumption that the scatter of the points excluding outliers (the effect of the median being to exclude outliers) would be represented by this minimum standard deviation. These minima were similar at each elevation, as expected, so we adopted their mean $(0.5 \times 10^{14}$ molecule cm$^{-2})$ and derived the standard error by dividing by the square root of the number of data points. Although the number differed significantly from day to day because of elimination of cloudy parts of days and changes in the length of daylight, they ranged from 7 on 25 August via 33 on 2 October to over 177 on 1 November, so the resultant standard errors were small. These standard errors are only the random component, systematic errors are not included.

5. Vertical profile inversion of MAX-DOAS data

AMFs at the different MAX-DOAS elevation angles have different sensitivities to absorbers at different heights. The higher the altitude of the absorber, the more similar are the AMFs, whereas for an absorber close to the surface, low elevations have much larger AMFs than those for high elevations.

This property can be used to invert a vertical profile of a set of MAX-DOAS measurements. We used the Bremen scheme detailed in Wittrock [31], which includes optimal estimation [32]. This scheme simultaneously fits to the O_4 and BrO measurements, as scattering by aerosol or thin-cloud, which strongly affects O_4 amounts, is an important part of the calculation. The inputs to the scheme are the solar zenith and azimuth angles, as well as the slant amounts of BrO and O_4 plus their random errors. These errors allow a calculation of the formal random error component of the inverted profile.

The trace of the averaging kernel, widely used as measure of the number of pieces of independent information in the profiles [32], has a mean value of 2.5, so we have assumed 3 pieces of information. Hence we vertically average the results from the programme grid of 0.05 km to correspond to approximate widths of averaging kernels (not shown), otherwise the results are unstable and give a false impression of the resolution. The averaging kernel centred at 0.2 km extends to between 300 and 500 m at half-height, so we chose to average from 0 to 400 m for the near-surface point. Other points, chosen from the widths of the averaging kernels at half height, are 0.4–0.8 km (centre 0.6 km) and 0.8–3.2 km (centre 2 km). There is little information above 3.5 km.

The inversion results in Fig. 7 show that many profiles have significant amounts of BrO above the lowest layers. The random error bars from the inversion are calculated by the inversion programme from the random errors in the
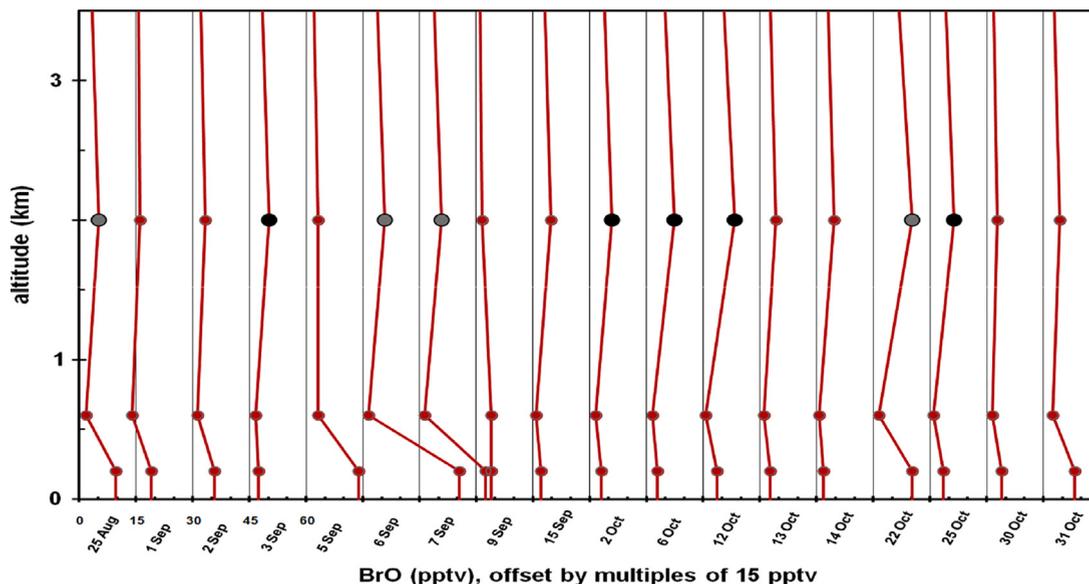
Fig. 7. Vertical profiles of BrO inverted from the MAX-DOAS data (see Section 5). Values have been vertically averaged over the altitude ranges for which the inversion has near-independent pieces of information, centred at 0.2, 0.6 and 2 km. Points with enhanced BrO aloft (>5 pptv at 2 km) are overlaid in black or grey (BrO at 0.2 km $<$ or >5 pptv, respectively). One-sigma error bar due only to the contribution from random error in each day's slant amounts (see text for calculation of errors in daily slant amounts) are too small to plot on this figure because of its poor horizontal resolution, but they are between 1 and 2 times the width of the symbols at 0.2 km (some exact values are given in Fig. 8 and Section 5), about equal to their width at 0.6 km, and about 1/2 the unoverlaid width at 2 km. Note that systematic errors are likely to be much larger, see text.
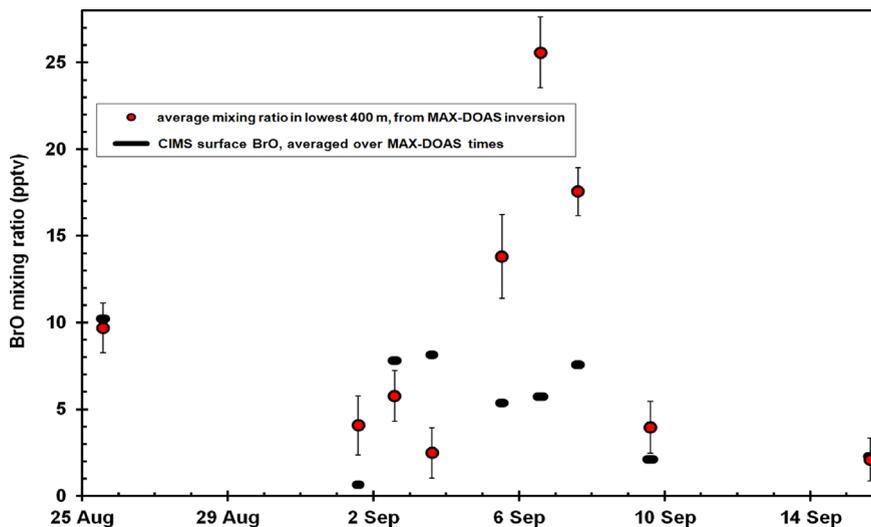
Fig. 8. Near-surface mixing ratios of BrO from the inversion of MAX-DOAS data, compared to the simultaneous in-situ measurements by the CIMS. Error bars on MAX-DOAS inversions are 1-sigma and are due only to the contribution from random error in each day's slant amounts; systematic errors are likely to be much larger. The ratio of the mean MAX-DOAS to mean CIMS values shown here is 1.7 ± 0.6, compared to the 10-fold disagreement in Fig. 4.

daily values of slant amounts (see the last paragraph in Section 4 for the calculation of random errors in daily slant amounts). The mapping of the random components of error from the input data to the inverted profiles, when using the inversion methodology of Rodgers [32], is too lengthy to be presented here; full details are given by Rodgers [32] and repeated by Wittrock [31, pp. 108–110], and it is a well-understood and extremely rigorous process. The random errors in inverted profiles are not plotted

in Fig. 7 as they are too small except at the lowest altitude, but at 2 km, the mean error for the whole data set was 0.5 pptv, and at 0.6 km it was 1.0 pptv (1-sigma). The mean value for the whole data set at 2 km is 5 pptv, almost 10 times the mean random error – the results at 2 km are highly significant. Furthermore, the a priori chosen was a simple linear one going from 2 pptv at the surface to 0.1 pptv at 6 km with assumed errors of 100%, so the inverted values are much larger than the a priori values
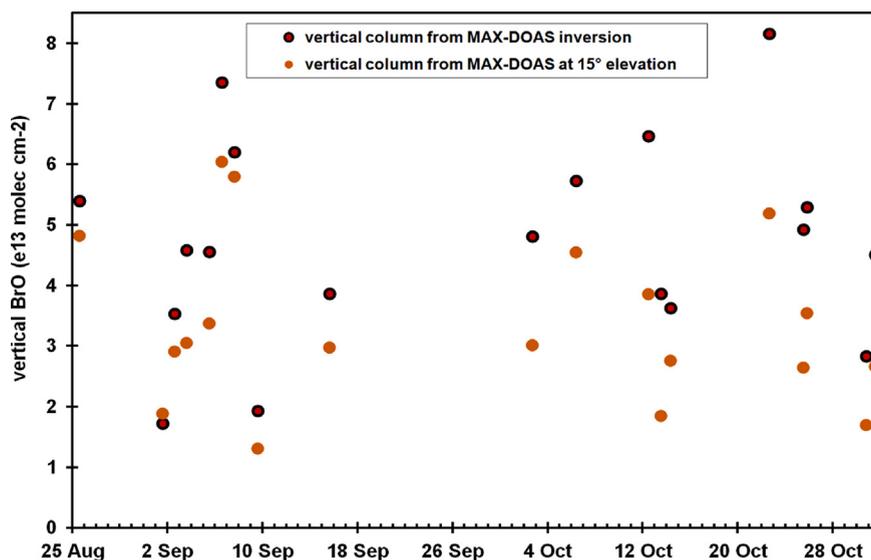
Fig. 9. Vertical amounts of BrO from the inversion of MAX-DOAS data, compared to the simple calculation of vertical amounts from the 15° elevation of MAX-DOAS data. The latter values are mostly smaller, suggesting consistent errors in the AMFs, unsurprising as they assumed all BrO to be near the surface.

plus assumed errors, another demonstration of the large information content of the inverted profiles above the lowest layers (see [32] for a discussion of information content when comparing inverted profiles to a-priori profiles). Off diagonal elements of the a priori covariance matrix were Gaussian functions chosen to give a correlation length of 25 m, following Barret et al. [33] and Hendrick et al. [34].

Note that systematic errors in inverted profiles, due to errors in cross sections and in aerosol, are not included here, and are likely to be much larger. However, errors in cross sections are likely to be similar on many days and at all altitudes. Furthermore, there was so little aerosol in the clean atmosphere of Antarctica that values of the aerosol optical depth from the inversion were always less than 0.1 (the resultant O_4 slant columns were always within the error bars of the measured O_4), so variation with altitude of the errors in the inverted profiles due to errors in aerosol is likely to be small. A full description of systematic errors in inverted BrO profiles must await a validation paper.

One component of error not included is that due to the off-diagonal elements of the covariance matrix calculated by the inversion programme. This will make a contribution to random error that depends on profile shape, so will vary with altitude and from day to day. Again, a full description of this error component must await a validation paper.

The mean inverted mixing ratio over the lowest 400 m is the best measure of the near-surface mixing ratio from the inversion, for comparison with CIMS data. Fig. 8 shows the results, which are much more convincing than those in Fig. 4: the ratio of the mean MAX-DOAS to mean CIMS values in Fig. 8 is 1.7 ± 0.6, compared to the 10-fold disagreement in Fig. 4. There is still disagreement in Fig. 8, which is to be expected as the vertical inversion cannot say whether there is less or more BrO at 10 m than at 300 m. Fig. 8 also demonstrates that the values of the random component of error from the inversion are believable.

The total vertical columns from the inversion programme should be better measures of total column than any of those from the slant columns at individual elevation angles (Fig. 5) or their mean (Fig. 2). The slant column at 15° elevation is the least dependent on the profile shape, but it still has some dependency. Fig. 9 shows that the vertical columns from the inversion programme range up to 8×10^{13} molecule cm^{-2}. It is reassuring that this is only slightly larger than the upper limit of 7×10^{13} molecule cm^{-2} from GOME-2 near Halley in spring 2007 [21].

6. Conclusion

There is a large discrepancy between remote-sensing and in-situ measurements of BrO during Antarctic enhancements episodes if the BrO is assumed to lie within a surface layer similar in thickness to that of the mixed layer. Possible sources of error identified in analysis of the MAX-DOAS results would make the disagreement worse. Our measurements can only be reconciled if large amounts of BrO are frequently at higher altitudes (i.e. in the free troposphere). The change of MAX-DOAS results with elevation angle supports this conclusion. Formal inversion of vertical profiles of MAX-DOAS BrO also shows large amounts at higher altitudes, and the inverted near-surface mixing ratios are of similar magnitude to the CIMS surface mixing ratios. Hence we conclude that large amounts of BrO frequently extend to several km altitude during Antarctic enhancement episodes, when up to 9/10 of the BrO can be above the mixed layer.

Perhaps we should not be surprised at this conclusion. BrO enhancements are often observed during storms, with surface winds that can exceed 15 m s^{-1} [35]. This must stir the atmosphere so vigorously that air must be lofted several km. Furthermore, Fig. 10 illustrates that many ozone depletion episodes show ozone loss in the free troposphere [3,36], often with back-trajectories that
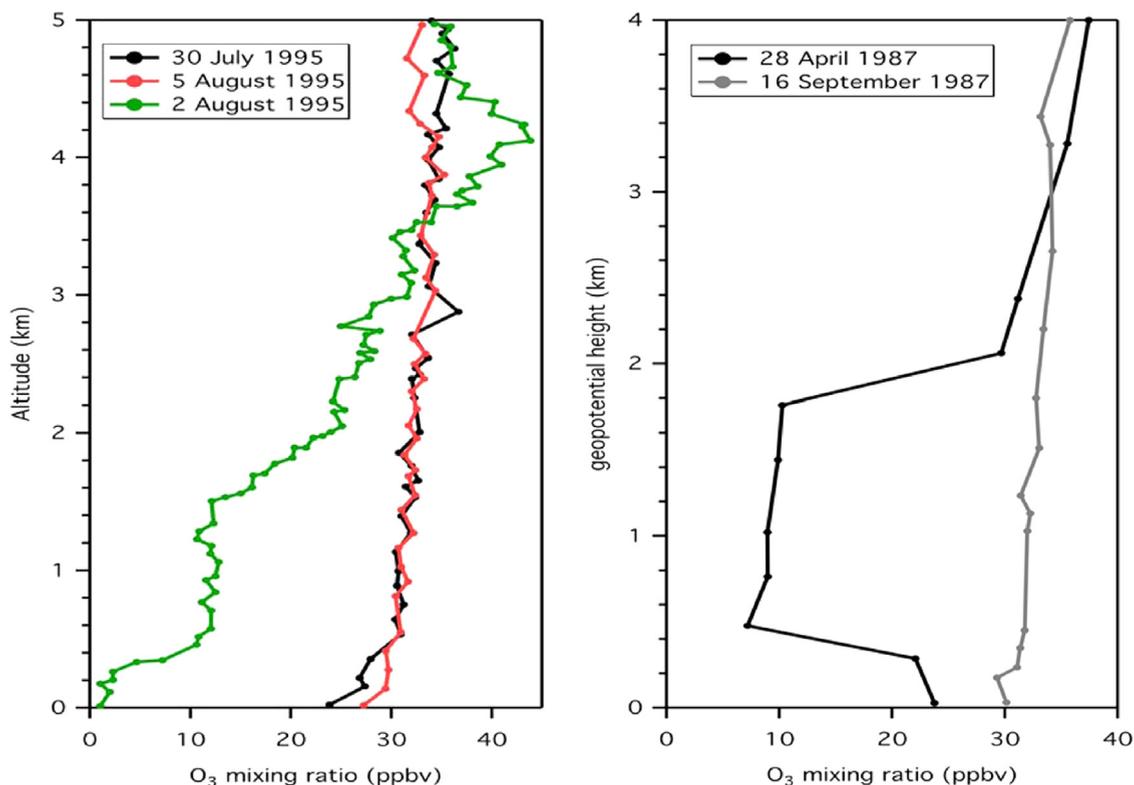
Fig. 10. Left: selected ozonesonde profiles measured in spring in Antarctica at Neumayer (71°S, 8°W) in 1995 [3], showing ozone depletion well above the 200–300-m thick mixed layer on one of the days. Right: as left but at Halley in 1987 [36].

showed air-mass contact with the surface 3–5 days earlier [3], this being the approximate lifetime of Bry in the absence of precipitation [37].

We conclude that the large apparent discrepancy between surface measurements of BrO mixing ratio and remote-sensing measurements of BrO vertical columns during enhancement episodes in Antarctica in 2007 is resolved by BrO being routinely but not universally present well above the surface during such episodes. This conclusion is consistent with other aspects of the remote-sensing measurements, and with other observations of BrO enhancement and ozone depletion episodes. Hence we recommend that future studies interpreting remote-sensing measurements of BrO during polar enhancements include the assumption that much of the BrO may be in the free troposphere.

References

[1] Simpson WR, von Glasow R, Riedel K, Anderson PS, Ariya P, Bottenheim J, et al. Halogens and their role in polar boundary-layer ozone depletion. Atmos Chem Phys 2007;7:4375–418.
[2] Fan SM, Jacob DJ. Surface ozone depletion in Arctic spring sustained by bromine reactions on aerosols. Nature 1992;359:522–4.
[3] Roscoe HK, Kreher K, Friess U. Ozone loss episodes in the free Antarctic troposphere, suggesting a possible climate feedback. Geophys Res Lett 2001;28:2911–4.
[4] McElroy CT, McLinden CA, McConnell JC. Evidence for bromine monoxide in the free troposphere during the Arctic polar sunrise. Nature 1999;397:338–40.
[5] Parrella JP, Chance K, Salawitch RJ, Canty T, Dorf M, Pfeilsticker K. New retrieval of BrO from SCIAMACHY limb: an estimate of the stratospheric bromine loading during April 2008. Atmos Meas Tech Discuss 2012;5:8017–50.
[6] Salawitch RJ, Canty T, Kurosu T, Chance K, Liang Q, da Silva A, et al. A new interpretation of total column BrO during Arctic spring. Geophys Res Lett 2010;37:L21805.
[7] Choi S, Wang Y, Salawitch RJ, Canty T, Joiner J, Zeng T, Kurosu TP, et al. Analysis of satellite-derived Arctic tropospheric BrO columns in conjunction with aircraft measurements during ARCTAS and ARCPAC. Atmos Chem Phys 2012;12:1255–85.
[8] Friess U, Sihler H, Sander R, Pöhler D, Yilmaz S, Platt U. The vertical distribution of BrO and aerosols in the Arctic: measurements by active and passive differential optical absorption spectroscopy. J Geophys Res 2011;116:D00R04.
[9] Hönninger G, Platt U. Observations of BrO and its vertical distribution during surface ozone depletion at Alert. Atmos Env 2002;36:2481–9.
[10] Prados-Roman C, Butz A, Deutschmann T, Dorf M, Kritten L, Minikin A, et al. Airborne DOAS limb measurements of tropospheric trace gas profiles: case studies on the profile retrieval of O₄ and BrO. Atmos Meas Tech 2011;4:1241–60.
[11] Neuman JA, Nowak JB, Huey LG, Burkholder JB, Dibb JE, Holloway JS, et al. Bromine measurements in ozone depleted air over the Arctic Ocean. Atmos Chem Phys 2010;10:6503–14.

[12] Jones AE, Wolff EW, Salmon RA, Bauguitte SJ-B, Roscoe HK, Anderson PS, et al. Chemistry of the Antarctic Boundary Layer and the Interface with Snow: an overview of the CHABLIS campaign. Atmos Chem Phys 2008;8:3789–803.

[13] Kurucz RL, Furenlid I, Brault J, Testerman L. Solar flux atlas from 296 nm to 1300 nm. National Solar Observatory Atlas No 1984;1.

[14] Wahner A, Ravishankara AR, Sander SP, Friedl RR. Absorption cross-section of BrO between 312 and 385 nm at 298 and 223 K. Chem Phys. Lett 1988;152:507–12.

[15] Aliwell SR, Van Roozendael M, Johnston PV, Richter A, Wagner T, et al. Analysis for BrO in zenith-sky spectra: an intercomparison exercise for analysis improvement. J Geophys Res 2002;107:D4199.

[16] Hönninger G, von Friedeburg C, Platt U. Multi axis differential optical absorption spectroscopy (MAX-DOAS). Atmos Chem Phys 2004;4:231–54.

[17] Mayer B, Kylling A. Technical note: the libRadtran software package for radiative transfer calculations – description and examples of use. Atmos Chem Phys 2005;5:1855–77.

[18] Hendrick F, Van Roozendael M, Kylling A, Petritoli A, Rozanov A, Sanghavi S, et al. Intercomparison exercise between different radiative transfer models used for the interpretation of ground-based zenith-sky and multi-axis DOAS observations. Atmos Chem Phys 2006;6:93–108.

[19] Roscoe HK, Van Roozendael M, Fayt C, du Piesanie A, Abuhassan N, Adams C, et al. Intercomparison of slant column measurements of NO_2 and O_4 by MaxDOAS and zenith-sky UV and visible spectrometers. Atmos Meas Tech 2010;3:1629–46.

[20] Munro R., Eisinger M., Anderson C., Callies J., Corpaccioli E., Lang R., et al. GOME-2 on Metop: from in-orbit verification to routine operations. In: Proceedings of the 2006 EUMETSAT meteorological satellite conference, Helsinki, Finland;12–16 June 2006. p. 48, 8711.

[21] Theys N, Van Roozendael M, Hendrick F, Yang X, De Smedt I, Richter A, et al. Global observations of tropospheric BrO columns using GOME-2 satellite data. Atmos Chem Phys 2011;11:1791–811.

[22] Theys N, Van Roozendael M, Errera Q, Hendrick F, Daerden F, Chabrillat S, et al. A global stratospheric bromine monoxide climatology based on the BASCOE chemical transport model. Atmos Chem Phys 2009;9:831–48.

[23] Saiz-Lopez A, Mahajan AS, Salmon RA, Bauguitte SJ-B, Jones AE, Roscoe HK, Plane JMC. Boundary layer halogens in coastal Antarctica. Science 2007;317:348–51.

[24] Huey LG, Dunlea EJ, Lovejoy ER, Hanson DR, Norton RB, Fehsenfeld FC, Howard CJ. Fast time response measurements of HNO_3 in air with a chemical ionization mass spectrometer. J Geophys Res 1998;103:3355–60.

[25] Slusher DL, Pitteri J, Haman BJ, Tanner DJ, Huey LG. A chemical ionization technique for measurement of Pernitric Acid in the upper troposphere and the Polar Boundary layer. Geophys Res Lett 2001;28:3875–8.

[26] Buys Z, Brough N, Huey LG, Tanner DJ, von Glasow R, Jones AE. High temporal resolution Br_2, $BrCl$ and BrO observations in coastal Antarctica. Atmos Chem Phys 2013;13:1329–43. http://dx.doi.org/10.5194/acp-13-1329-2013.

[27] Slusher DL, Tanner DJ, Flocke FM, Roberts JM. A thermal dissociation chemical ionization mass spectrometry (TD-CIMS) technique for the simultaneous measurement of peroxyacyl nitrates and dinitrogen pentoxide. J Geophys Res 2004;109. http://dx.doi.org/10.1029/2004JD004670.

[28] Liao J, Sihler H, Huey LG, Neuman JA, Tanner DJ, Friess U, et al. A comparison of Arctic BrO measurements by chemical ionisation mass spectrometry and long path-differential optical absorption spectroscopy. J Geophys Res 2011;116D00R02 2011;116.

[29] Wagner T, Ibrahim O, Sinreich R, Frieß U, von Glasow R, Platt U. Enhanced tropospheric BrO over Antarctic sea ice in mid winter observed by MAX-DOAS on board the research vessel Polarstern. Atmos Chem Phys 2007;7:3129–42.

[30] Anderson PS, Neff WD. Boundary layer physics over snow and ice. Atmos Chem Phys 2008;8:3563–82.

[31] Wittrock F. The retrieval of oxygenated volatile organic compounds by remote sensing techniques [Ph.D. thesis]. University of Bremen. ⟨http://www.doas-bremen.de/paper/diss_wittrock_06.pdf⟩; May 2006 [last accessed January 2014].

[32] Rodgers CD. Characterization and error analysis of profiles retrieved from remote sounding measurements. J Geophys Res 1990;95:5587–95.

[33] Barret B, De Maziere M, Demoulin P. Retrieval and characterization of ozone profiles from solar infrared spectra at the Jungfraujoch. J Geophys Res 2002:107. http://dx.doi.org/10.1029/2001JD001298.

[34] Hendrick F, Barret B, Van Roozendael M, Boesch H, Butz A, De Maziere M, et al. Retrieval of nitrogen dioxide stratospheric profiles from ground-based zenith-sky UV visible observations: validation of the technique through correlative comparisons. Atmos Chem Phys 2004;4:2091–106.

[35] Jones AE, Anderson PS, Begoin M, Brough N, Hutterli MA, Marshall GJ, et al. BrO, blizzards, and drivers of polar tropospheric ozone depletion events. Atmos Chem Phys 2009;9:4639–52.

[36] Jones AE, Anderson PS, Wolff EW, Roscoe HK, Marshall GJ, Richter A, Brough N, Colwell SR. Vertical structure of Antarctic tropospheric ozone depletion events: characteristics and broader implications. Atmos Chem Phys 2010;10:7775–94.

[37] Yang X, Pyle JA, Cox RA, Theys N, Van Roozendael M. Snow-sourced bromine and its implications for polar tropospheric ozone. Atmos Chem Phys 2010;10:7763–73.